Anisotropic Superconducting Properties of Aligned MgB_2 Crystallites

O. F. de Lima, R. A. Ribeiro, M. A. Avila, C. A. Cardoso, and A. A. Coelho
Instituto de Física "Gleb Wataghin," UNICAMP, 13083-970, Campinas, SP, Brazil
(Received 15 March 2001)

Samples of aligned MgB_2 crystallites have been prepared, allowing for the first time the direct identification of an upper critical field anisotropy $H_{c2}^{ab}/H_{c2}^{c} = \xi_{ab}/\xi_c \simeq 1.7$, with $\xi_{o,ab} \simeq 70$ Å, $\xi_{o,c} \simeq 40$ Å, and a mass anisotropy ratio $m_{ab}/m_c \simeq 0.3$. A ferromagnetic background signal was identified, possibly related to the raw materials purity.

DOI: 10.1103/PhysRevLett.86.5974 PACS numbers: 74.25.Ha, 74.60.Ec, 74.60.Jg, 74.70.Ad

The recent discovery of superconductivity at 39 K in magnesium diboride (MgB_2) [1] has brought new excitement to the area of basic and applied research on superconducting materials. The observation of an isotope effect [2], a BCS-type energy gap measured by scanning tunneling spectroscopy [3], as well as band structure studies [4,5], points to a phonon-mediated superconductivity in MgB_2. Some reports [6,7] have suggested that MgB_2 has an isotropic (or 3D) behavior, based on measurements done in polycrystalline samples. However, other studies [8,9] have also discussed its possible anisotropic nature. The relatively high values reported for the critical current density [6,10] (J_c) are possibly indicating the absence of weak link problems, which are well known in the high-T_c materials. While polycrystalline MgB_2 is very easy to grow and is a readily available reagent, good-sized single crystals of this material have not yet been reported, and their development promises to be a greater challenge. Here we present results from samples of aligned MgB_2 crystallites that establish the anisotropy of the upper critical field (H_{c2}), thus implying an anisotropic character for other superconducting properties, e.g., the energy gap, coherence length (ξ), field penetration depth (λ), and J_c.

In this work, a weakly sintered sample of MgB_2 was prepared, starting with a stoichiometric mixture of 99.5 at. % pure boron and 99.8 at. % pure magnesium, both in chips form (Johnson Matthey Electronics). The loose mixture was sealed in a Ta tube under Ar atmosphere, which was then encapsulated in a quartz ampoule and put into the furnace. The compound formation was processed by initially holding the furnace temperature at 1200 °C for 1 h, followed by a decrease to 700 °C (10 °C/h), then to 600 °C (2 °C/h), and finally to room temperature at a rate of 100 °C/h. The weakly sintered product was easily crushed and milled employing mortar and pestle. Using a stereomicroscope we could observe a very uniform powder consisting mainly of shiny crystallites, with aspect ratios ranging from 2 to 5. This is mainly due to the main surface size distribution ranging from 5 to 40 μm for the larger linear dimension, since the crystallites' thickness is very regular, around 2 μm. The powder was then sieved into a range of particle sizes between 5–20 μm, which allows the crystallites fraction to be maximized to almost 100%. Small amounts of the powder were then patiently spread on both sides of a small piece of paper, producing an almost perfect alignment of the crystallites, as shown in the scanning electron microscopy (SEM) picture in the upper part of Fig. 1. The lower part of this figure shows an x-ray diffraction pattern (θ-2θ scan) from a sample of the *crystallite-painted* paper, displaying only the (001) and (002) reflections coming from the MgB_2 phase. A lattice parameter $c = 3.518 \pm 0.008$ Å was evaluated from these two peak positions. The two small impurity peaks marked with asterisks were indexed as SiO_2. The inset in Fig. 1

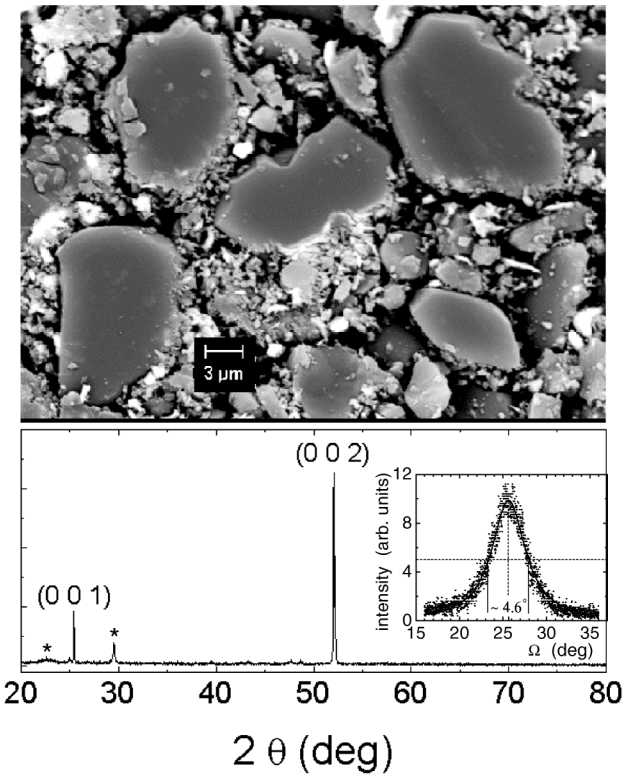

FIG. 1. Top: SEM picture showing the well aligned crystallites and intercrystallite material. Bottom: x-ray diffraction pattern showing only the (001) and (002) peaks of MgB_2, plus two spurious peaks indexed as SiO_2. Inset: rocking curve (ω scan) for the (002) peak, showing an angular spread of about 4.6° along the crystallites' c axis.

 0031-9007/01/86(26)/5974(4)$15.00

shows a rocking curve (ω scan) for the (002) peak that reveals an angular spread around 4.6°, associated with a small misalignment of the crystallites' c axis.

Electron microprobe analysis done on four different areas between the MgB_2 crystallites revealed the following average concentration (in at. %) of elements: O (62.9), C (22.2), Ca (9.48), Si (1.48), Mg (1.44), Al (1.37), K (0.09), Fe (0.50), Cr (0.21), and Ni (0.09). The first eight elements in this list were found also in the composition analysis made on the same type of paper used (Canson, ref. 4567-114). Microprobe analysis done also on the initial Mg and B revealed a few small precipitates, smaller than 10 μm and containing up to 8 at. % Fe, only in the Mg chips. This confirms the expectation of Fe being a common impurity [11] in commercial Mg and sets a general concern on its possible effects. The average composition found on top of several crystallites, normalized to the whole MgB_2 formula unit, was Mg (30.80), O (2.20), Ca (0.17), Si (0.07), and Fe (0.06). Although boron contributes with a fraction of 66.6 at. %, it does not show up in the microprobe analysis because it is too light. The contaminants found on top of the crystallites most possibly came from a surface contamination caused by the alignment technique, which required vigorous rubbing on top of the powder, using a steel tweezers tip to spread the crystallites uniformly. This is corroborated by a further analysis done on top of several as-grown crystallites, which detected only Mg and a small amount of O (possibly from MgO). This result is consistent with the very small solid solubility limit of about 0.004 at. % Fe in Mg, which is known to occur [12] at the solidification temperature of 650 °C. The intercrystallite type of *rubbish* shown in Fig. 1 is attributed mainly to the paper abrasion, which produces a varied distribution of irregular grains of paper fragments. In order to characterize the superconducting and magnetic properties of the aligned crystallites, we mounted several samples consisting of a pile of five small squares (3×3 mm^2) cut from the *crystallite-painted* paper and glued with Araldite resin. Each one of these samples contains a number of crystallites estimated to be around 6.5×10^5, totalizing an effective volume of 0.065 mm^3, which is reasonably close to 0.060 mm^3 that was evaluated from the expected slope of $-1/4\pi$ for the diamagnetic shielding at $H \approx 0$.

Figure 2 shows the anisotropic signature of the $H_{c2}(T)$ line in the field interval $0 \leq H \leq 40$ kOe. The values were taken from the transition onset of the real component (χ') of ac susceptibility, measured using a PPMS-9T machine (Quantum Design), with an excitation field of amplitude 1 Oe and frequency 5 kHz. The inset shows an enlarged view of the $\chi'(T)$ curves for $H \parallel ab$ (open symbols) and $H \parallel c$ (solid symbols), the field orientation parallel to the ab plane and parallel to the c axis, respectively. The $\chi'(T)$ as well as the $M(T)$ (inset of Fig. 3) measurements, for $H = 10$ Oe, show sharp transitions at the same critical temperature $T_c = 39.2$ K. The dashed lines connecting points in Figs. 2–4 are only guides to the eyes.

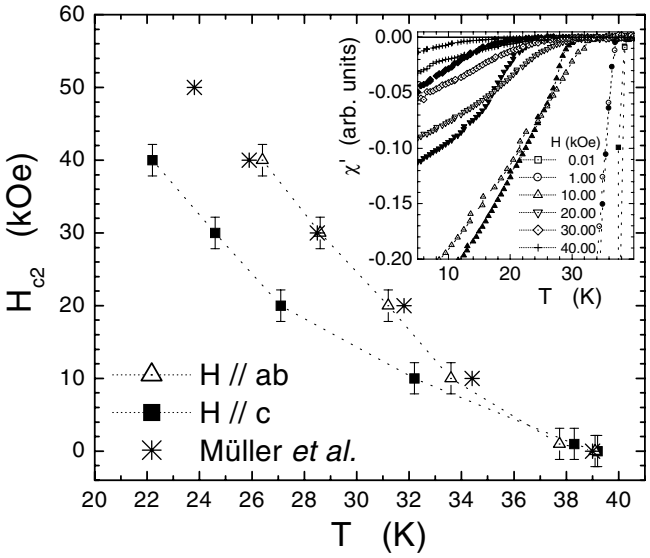

FIG. 2. Upper critical field H_{c2} vs temperature phase diagram, for both sample orientations. The stars represent the H_{c2} vs T line from Ref. [13]. The inset shows the real component χ' of the ac susceptibility vs temperature, measured at several dc fields for both orientations. Open symbols are for the $H \parallel ab$ curves and solid symbols for $H \parallel c$.

Typically, some of the published data on the temperature dependence [2,10,13,14] of $H_{c2}(T)$ agree with our result for $H_{c2}(T) \parallel ab$. As an example, the data from Ref. [13] are plotted in Fig. 2 as stars. This could simply mean that in polycrystalline samples the transitions are broadened, showing the onset at the highest temperature that corresponds to the highest critical field available, which is $H_{c2}(T) \parallel ab$.

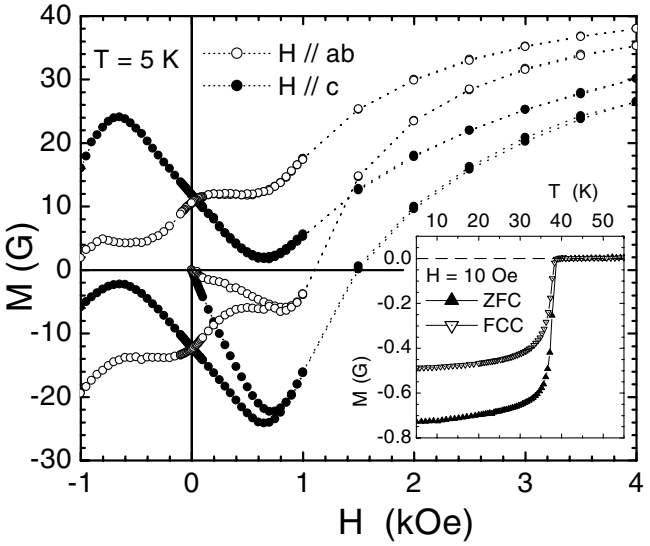

FIG. 3. Magnetization loops at 5 K for both sample orientations, showing a superconducting hysteresis on a ferromagnetic background. The inset shows a zero field cooling (ZFC) and a field cooling measured on cooling (FCC) magnetization curve for $H = 10$ Oe. We see a sharp transition at $T_c = 39.2$ K and a relatively high (~70%) recovery of diamagnetism for the FCC curve.

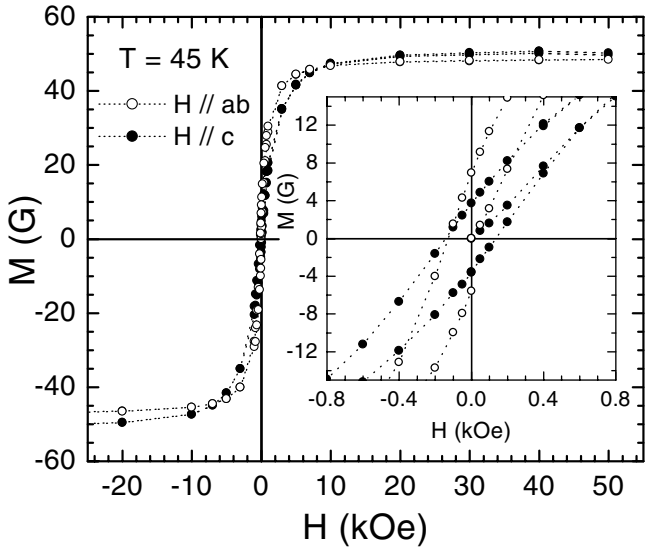

FIG. 4. Magnetization loops at 45 K (above T_c) for both sample orientations, showing the ferromagnetic behavior of our sample. The inset shows the hysteretic behavior at low fields.

The ratio $\eta = H_{c2}^{ab}/H_{c2}^{c}$, between the upper critical field when H is applied parallel to the ab plane, and when it is along the c direction, was evaluated at different temperatures, producing $\eta = 1.73 \pm 0.03$. Using the Ginzburg-Landau mean field expression [15] $\xi(T) = \xi_o(1 - T/T_c)^{-1/2}$ and the results for anisotropic situations [16,17] $H_{c2}^{c}(T) = \phi_o/(2\pi\xi_{ab}^2)$ and $H_{c2}^{ab}/H_{c2}^{c} = 1/\varepsilon$, where $\phi_o = 2.07 \times 10^{-7}$ G cm^2 is the quantum of flux (in CGS units) and $\varepsilon^2 = m_{ab}/m_c$ is the mass anisotropy ratio, we find that $\xi_{o,ab}/\xi_{o,c} = \xi_{ab}(T)/\xi_c(T) = \eta \simeq 1.73$ and $\varepsilon^2 \simeq 0.3$. Since at $T = 27$ K we have $H_{c2}^{c} = 20$ kOe, this implies that $\xi_{o,ab} \simeq 70$ Å and $\xi_{o,c} \simeq 40$ Å. The mass anisotropy ratio of MgB_2 thus corresponds to a relatively small anisotropy when compared to the highly anisotropic high-T_c cuprates [17], such as $YBa_2Cu_3O_7$ ($\varepsilon^2 \simeq 0.04$) and $Bi_2Sr_2CaCu_2O_8$ ($\varepsilon^2 \simeq 10^{-4}$). We do not expect that a likely very small bulk contamination of the crystallites could eventually change their anisotropy values. In fact, our careful composition analysis has indicated that almost all contaminants are located in the region between the crystallites, thus having a negligible chance to affect the underlying mechanism of the superconducting condensation.

The magnetization curves $M(T)$ and $M(H)$, displayed in Figs. 3 and 4, were measured using a SQUID magnetometer (Quantum Design, model MPMS-5). The $M(H)$ curves ($T = 5$ K) shown in Fig. 3 are intriguing in the region $-1 \lesssim H \lesssim 1$ kOe, where the maximum shielding and first field penetration (in the initial virgin state) occur. For $|H| \gtrsim 1$ kOe the hysteretic curves in both field directions look very similar. However, for $|H| \gtrsim 40$ kOe (not shown here) the magnetization difference between the up and down curves (ΔM) becomes smaller than the noise. Large fluctuations of the magnetic moment were consistently observed in this field region, for three different samples and temperatures ($T = 5, 10, 20$ K), possibly associated with the high creep rate and the fast drop of J_c occurring at high fields [10,14,18,19]. Figure 4 shows a clear signature of the ferromagnetic hysteresis loop measured at $T = 45$ K, mainly attributed to the presence of Fe, Cr, and Ni in the intercrystallite region. The inset displays an enlarged view close to $H = 0$ indicating that demagnetization effects are also observed for the $H \parallel ab$ and $H \parallel c$ orientations. In a recent detailed study [8] the occurrence of Fe contamination has already been identified, through measurements of MgB_2 samples made from commercial powder supplied by a different company.

In view of the superimposed ferromagnetic signal in the magnetization curves, we found it to be not reliable to discuss the expected anisotropy in $J_c \propto \Delta M$, which could be determined using the Bean model [20]. A rough estimate for both field orientations gives $J_c \simeq 10^6$ A/cm^2 at $H = 1.5$ kOe and $T = 5$ K (Fig. 3). This calculation neglects the small influence of the ferromagnetic hysteresis and considers the average crystallite geometry as described before. However, an anisotropy between $J_c(H \parallel c)$ and $J_c(H \parallel ab)$ should be expected. Indeed, independently of the different regime of vortex pinning, J_c is predicted [17] to be proportional to ξ^2, leading to $J_c(H \parallel c)/J_c(H \parallel ab) \approx (\xi_{ab}/\xi_c) \approx H_{c2}^{ab}/H_{c2}^{c}$.

A final cautionary observation has to be addressed to the possibility that surface superconductivity could also be occurring for $H \parallel ab$, since coincidently the surface nucleation field is [21] $H_{c3} \simeq 1.7 H_{c2}$. However, we have made several careful measurements of $M(H)$ and $\chi'(H)$, as well as $M(T)$ and $\chi'(T)$, around the onset of transition, and no signature [22] of a surface nucleation field was found. This is consistent with the fact that our $H_{c2}^{ab}(T)$ line agrees with several reported $H_{c2}(T)$ lines measured in polycrystalline samples [2,10,13,14], which certainly did not comply with the boundary condition [21,22] required for surface nucleation in the ab planes, i.e., $H \parallel ab$.

In conclusion, we have prepared samples of aligned MgB_2 crystallites that allowed, for the first time, the identification of an anisotropy for the upper critical field given by $H_{c2}^{ab}/H_{c2}^{c} \simeq 1.73$, implying an anisotropy of the coherence length $\xi_{ab}/\xi_c \simeq 1.73$ and a mass anisotropy ratio $m_{ab}/m_c \simeq 0.3$. This could be considered a mild anisotropy when compared to the values found for the high-T_c materials ($m_{ab}/m_c \lesssim 0.04$). The influence of contaminants is requiring further work, aimed at a more complete and reliable characterization of the MgB_2 intrinsic properties. Naturally the production of a good-sized single crystal of MgB_2 is also highly desirable.

We are very grateful to S. Gama for supplying some of the raw materials, to I. Torriani and C. M. Giles for the x-ray diffractograms, and to D. Silva (IG-Unicamp) for the SEM and microprobe analysis. This work is supported by the Brazilian science agencies FAPESP (Fundação de Amparo a Pesquisa do Estado de São Paulo) and CNPq (Conselho Nacional de Desenvolvimento Científico e Tecnológico).

Note added.—Since this manuscript was submitted two papers have appeared [23,24] showing results consistent with our anisotropy data.

[1] J. Akimitsu, in Proceedings of the Symposium on Transition Metal Oxides, Sendai, 2001 (to be published); J. Nagamatsu *et al.,* Nature (London) **410**, 63 (2001).
[2] S. L. Bud'ko *et al.,* Phys. Rev. Lett. **86**, 1877 (2001).
[3] G. Karapetrov *et al.,* cond-mat/0102312.
[4] J. Kortus *et al.,* cond-mat/0101446 v2.
[5] N. I. Medvedeva *et al.,* cond-mat/0103157.
[6] D. C. Larbalestier *et al.,* Nature (London) **410**, 186 (2001).
[7] W. N. Kang *et al.,* cond-mat/0103161.
[8] Y. Wang, T. Plackowski, and A. Junod, cond-mat/0103181.
[9] J. M. An and W. E. Pickett, cond-mat/0102391 v2.
[10] P. C. Canfield *et al.,* Phys. Rev. Lett. **86**, 2423 (2001).
[11] G. V. Raynor, *The Physical Metallurgy of Magnesium and Its Alloys* (Pergamon, London, 1959), p. 441.
[12] *Binary Alloy Phase Diagrams,* edited by T. B. Massalski (ASM International, Materials Park, OH, 1990), 2nd ed., p. 1076.
[13] K.-H. Müller *et al.,* cond-mat/0102517.
[14] D. K. Finnemore *et al.,* Phys. Rev. Lett. **86**, 2420 (2001).
[15] M. Tinkham, *Introduction to Superconductivity* (McGraw-Hill, New York, 1996).
[16] L. N. Bulaevskii, V. L. Ginzburg, and A. A. Sobyanin, Zh. Eksp. Teor. Fiz. **94**, 355 (1988) [Sov. Phys. JETP **68**, 1499 (1988)].
[17] G. Blatter *et al.,* Rev. Mod. Phys. **66**, 1125 (1994).
[18] Y. Bugoslavsky *et al.,* Nature (London) **410**, 563 (2001).
[19] H. H. Wen *et al.,* cond-mat/0102436 v3.
[20] C. P. Bean, Rev. Mod. Phys. **36**, 31 (1964).
[21] D. Saint-James and P. G. de Gennes, Phys. Lett. **7**, 306 (1963).
[22] D. Saint-James, G. Sarma, and E. J. Thomas, *Type II Superconductivity* (Pergamon, Oxford, New York, 1969).
[23] A. Handstein *et al.,* cond-mat/0103408.
[24] F. Bouquet *et al.,* cond-mat/0104206.